

MOL #103127

Title Page

Temperature effects on kinetics of Kv11.1 drug block have important consequences for *in silico* proarrhythmic risk prediction.

Monique J. Windley, Stefan A. Mann, Jamie I. Vandenberg, Adam P. Hill

Victor Chang Cardiac Research Institute, 405 Liverpool Street, Darlinghurst, NSW 2010,
Australia (MW, SM, JV, AH)

St Vincent's Clinical School, University of NSW, Victoria Street, Darlinghurst, NSW 2010,
Australia (MW, SM, JV, AH)

MOL #103127

Running Title Page

Running title: Temperature dependent block of K_v11.1

Corresponding author:

Adam Hill

Molecular Cardiology and Biophysics Division

Victor Chang Cardiac Research Institute

405, Liverpool Street

Darlinghurst

NSW 2010

Australia

T: +61 2 9295 8686

F: +61 2 9295 8770

E: a.hill@victorchang.edu.au

Pages: 42

Tables: 4

Figures: 7

References: 32

Abstract words: 250

Introduction words: 738

Discussion words: 1500

MOL #103127

Abbreviations: AP, action potential; APD, action potential duration; $I_{Kv11.1}$, $K_v11.1$ channel current; I_{Kr} , rapid component of delayed rectifier current; ECG, electrocardiogram; C_{max} , maximum serum concentration; FDA, US Food and Drug Administration; CiPA, Comprehensive *In vitro* Proarrhythmic Assay, hERG, human Ether-à-go-go-related gene channel; RT, room temperature; CHO, Chinese hamster ovary; DMSO, dimethylsulfoxide; D + C, drug unbound channel; DC*, drug bound conducting channel; DC drug bound blocked channel.

MOL #103127

Abstract

Drug block of $K_v11.1$ (hERG) channels, encoded by the *KCNH2* gene, is associated with reduced repolarization of the cardiac action potential and is the predominant cause of acquired long QT syndrome that can lead to fatal cardiac arrhythmias. Current safety guidelines require that potency of $K_v11.1$ block is assessed in the preclinical phase of drug development. However, not all drugs that block $K_v11.1$ are proarrhythmic, meaning that screening based on equilibrium measures of block can result in high attrition of potentially low risk drugs. The next generation of drug screening approaches are set to be based around *in silico* risk prediction, informed by *in vitro* mechanistic descriptions of drug binding, including measures of the kinetics of block. A critical issue in this regard is characterizing the temperature dependence of drug binding. Specifically, it is important to address whether kinetics relevant to physiological temperatures can be inferred or extrapolated from *in vitro* data gathered at room temperature in high throughput systems. Here we present the first complete study of the temperature dependent kinetics of block and unblock of a proarrhythmic drug, cisapride, to $K_v11.1$. Our data highlight a complexity to binding that manifests at higher temperatures that can be explained by accumulation of an intermediate, non-productively bound, encounter complex. These results suggest that for cisapride, physiologically relevant kinetic parameters cannot be simply extrapolated from those measured at lower temperatures, but rather data gathered at physiological temperatures should be used to constrain *in silico* models that may be used for proarrhythmic risk prediction.

MOL #103127

Introduction

K_v11.1 channels are the pore forming subunit that conduct the rapid component of the delayed rectifier current (I_{Kr}) in the heart, one of the major contributors to cardiac repolarization (Sanguinetti et al., 1995). K_v11.1 is the target for the majority of drugs that cause drug-induced, or acquired long QT syndrome (Wood and Roden, 2004) that is characterised by prolonged QT interval on the electrocardiogram (ECG) and an increased risk of the potentially fatal ventricular arrhythmia torsades de pointes. As a result, preclinical safety guidelines stipulate that all drugs must be tested against K_v11.1 to assess proarrhythmic risk (ICH S7B, Food and Drug Administration, 2005). One method adopted in long QT risk assessment is the use of a provisional safety margin. The safety index value directly compares the electrophysiological determined IC₅₀ of K_v11.1 block to the maximum serum concentration (C_{max}) of the drug, such that the closer the values are the higher the proarrhythmic risk (Redfern et al., 2003). However, while these equilibrium measures of K_v11.1 are very sensitive (no new drugs have been withdrawn from the market due to proarrhythmic activity since the inception of these guidelines), they are not specific. Not all drugs that block K_v11.1 are proarrhythmic, resulting in a high attrition rate of potentially low risk drugs (Redfern et al., 2003; Sager et al., 2014; Yap and Camm, 2003). Furthermore, factors in addition to K_v11.1 block such as multichannel pharmacology or augmentation of the persistent sodium current via phosphoinositide 3-kinase (Yang et al. 2014), may also contribute to proarrhythmia. There is therefore widespread concern that the development of potentially useful therapeutics is being prematurely and unnecessarily terminated (Fermini et al., 2015; Sager et al., 2014).

MOL #103127

To tackle this issue, the US Food and Drug administration (FDA) has recently initiated the comprehensive *in vitro* proarrhythmic assay (CiPA) initiative that is tasked with developing a new approach to assigning risk to drugs in development. It focusses on actual markers of proarrhythmia, rather than indirect measures, such as $K_v11.1$ block, that may be poor surrogates for actual arrhythmic risk (Fermini et al., 2015; Sager et al., 2014). One of the major focusses of this initiative is the detailed *in vitro* mechanistic characterization of the effect of drugs on $K_v11.1$ as well as other channels, including $Na_v1.5$, $Ca_v1.2$, $K_v4.3$ with KChIP2, KCNQ1 with KCNE1 and Kir2.1 (Fermini et al., 2015). This information will be used to constrain *in silico* models of the action potential that can be used for computational risk prediction based on established proarrhythmic metrics such as early after depolarizations (EADs). Central to this mechanistic characterization is a growing appreciation that the kinetics of drug block, rather than just measures of potency may also be important in determining the amount of action potential duration (APD) prolongation and the degree of risk (Di Veroli et al., 2014; Fermini et al., 2015; Lee et al., 2015; Romero et al., 2014).

Given this understanding of the need to measure the kinetics of drug block, an important factor to consider is the temperature at which these data are gathered. Under current regulations, there are no guidelines specifying the temperature at which IC_{50} measurements are taken, however it has been established that the values obtained at room versus physiological temperatures can vary significantly for many drugs (Kirsch et al., 2004; Yao et al., 2005). From a practical perspective, many high throughput patch clamp platforms, that will be the mainstay of gathering this kinetic data within the pharmaceutical industry, are limited to recording at room temperature (RT) (Fermini et al., 2015). There is therefore considerable interest in addressing the question as to whether kinetic data

MOL #103127

gathered at lower temperatures could be easily extrapolated to physiological temperatures, or whether more detailed characterization must be carried out at physiological temperatures *in vitro*.

Here, we present the first full characterization of the temperature dependence of kinetics of block and unblock of a proarrhythmic drug, cisapride, to K_v11.1. Our results show that while IC₅₀ was independent of temperature, the kinetics of block and unblock were temperature dependent. Furthermore, our data reveal a complexity to cisapride block that we demonstrate, using *in silico* modelling, arises from accumulation of an intermediate encounter complex at higher temperatures. These findings suggest that, at least for cisapride, it is not possible to simply extrapolate from room temperature data to derive physiologically relevant block kinetics and that 37 °C *in vitro* data should be obtained to constrain physiologically relevant models for risk prediction.

MOL #103127

Materials and Methods

Cell culture

CHO cells stably expressing K_v11.1 were purchased from the American Type Culture Collection (ATCC reference PTA-6812). Cells were cultured in Hams F12 nutrient mix (ThermoFisher Scientific, Waltham, USA) containing 5% fetal bovine serum (Sigma-Aldrich, Sydney, Australia) and maintained at 37 °C with 5% CO₂.

Patch-clamp electrophysiology

Whole cell patch clamp currents were evoked from CHO cells in the voltage clamp configuration at 22, 27, 32 and 37 °C. The current signal was amplified and filtered at 1 kHz with an Axopatch200B (Molecular Devices, Sunnyvale, USA) and sampled at 4 kHz with a PC interfaced with an analog to digital converter, Digidata1440A (Molecular Devices). Leak currents were subtracted manually offline and series resistance compensation was >80%. Data was acquired with pCLAMP 10 (Molecular Devices) acquisition software and analysed using Clampfit (Molecular Devices) and Prism (v6, GraphPad, San Diego, USA).

Single use patch pipettes were pulled from borosilicate glass (Harvard Apparatus, Holliston, USA) with resistances of 2-5 MΩ. Pipettes were filled with internal solution containing (in mM): 120 potassium gluconate, 20 KCl, 1.5 Mg₂ATP, 5 EGTA and 10 HEPES, adjusted to pH 7.2 with KOH. The external bath solution contained (in mM); 130 NaCl, 5 KCl, 1 MgCl₂, 1 CaCl₂, 12.5 glucose and 10 HEPES, adjusted to pH 7.4 with NaOH. The calculated liquid junction potential of -15 mV (Barry, 1994) was corrected for by adjusting

MOL #103127

voltage pulse protocols prior to stimulation. All chemicals were purchased from Sigma-Aldrich (Sydney, Australia) unless otherwise stated.

Cisapride was delivered via a microfluidic device (Dynaflow Resolve, Celectricon, Mölndal, Sweden) with solution exchange time of <30 ms (Hill et al., 2014). The reusable Dynaflow system enabled delivery of discrete solutions of various drug concentrations under laminar flow. Temperature control was achieved using the Dynaflow Resolve heat control system (Celectricon, Sweden) allowing precise control of the solution temperature up to 45 °C. Temperature control was also validated by placing a temperature probe in the approximate position of the cell under patch clamp.

Cisapride was purchased from Sigma Aldrich and dissolved in DMSO with maximum final concentration of 0.0012% (v/v) in recording solution. The final concentration of DMSO was well below the 0.1% (v/v) shown to have no effect on K_V11.1 channel activity (Walker et al., 1999).

Data analysis

For analysis of drug block kinetics, exponential fits of current traces were performed using clampfit. Time constants of cisapride block and unblock were derived by fitting standard exponential equations to the raw current traces such that:

$$f(t)_{on} = (I_m - I_d) \times (e^{-t/\tau_{on}}) + I_d \quad \text{Eqn 1}$$

$$f(t)_{off} = (I_m - I_d) \times (1 - e^{-t/\tau_{off}}) + I_d \quad \text{Eqn 2}$$

MOL #103127

Where I_m is the maximum current amplitude, I_d is the current plateau amplitude in the presence of drug, t is time, τ is the time constant.

For analysis of steady state dose response, data were fit by the Hill equation:

$$y = \frac{1}{1 + ([x]/IC_{50})^{n_H}} \quad \text{Eqn 3}$$

where $[x]$ is cisapride concentration, n_H is the Hill coefficient (slope parameter), and IC_{50} is the concentration at which 50% block of channel current is evident.

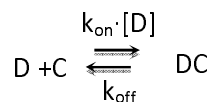
Statistical analyses were performed in Prism. ANOVA were used for statistical analysis between normally distributed data multiple groups of data with Tukey's post-hoc analysis of means for multiple comparisons and the Kruskal-Wallis test with Dunn's post-hoc analysis for multiple comparisons was used for non-normally distributed data. The Mann Whitney test was used for statistical analysis between two non-normally distributed data sets. P values < 0.05 were considered significant.

Modelling

Models of drug block kinetics were implemented as systems of coupled ordinary differential equations in Matlab 2015b, using the symbolic math toolbox. Sum of squares errors were calculated to evaluate the goodness of fit to the experimental data traces, and minimized using the fmincon solver that ships with Matlab (Mathworks, Natick, USA).

MOL #103127

Two schemes were considered to describe drug block. First, a simple bimolecular interaction:



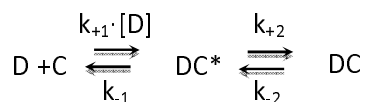
Scheme 1

Where D is the drug, C is the channel and DC is the drug bound, blocked channel. The rates of drug association (forward rate, k_{on}) and dissociation (reverse rate, k_{off}) were calculated directly from the measured τ values as follows:

$$k_{off} = 1/\tau_{off} \quad \text{Eqn 4}$$

$$k_{on} = \frac{(1/(\tau_{on} - k_{off}))}{[D]} \quad \text{Eqn 5}$$

The second scheme that was used to describe the data incorporated an intermediate encounter complex:



Scheme 2

MOL #103127

Where DC* is the encounter complex representing a drug bound, conducting state. Scheme 2 was fit to idealized traces representing the timecourse of block and unblock of cisapride (calculated from the averaged τ_{on} , τ_{off} values and percentage block under each dose and temperature condition) to yield values for the forward rates of transition between the states k_{+1} and k_{+2} and reverse rates, k_{-1} and k_{-2} . Equilibrium constants for individual transitions of Scheme 2 were calculated as:

$$K_1 = k_{+1}/k_{-1} \quad \text{Eqn 6}$$

and

$$K_2 = k_{+2}/k_{-2} \quad \text{Eqn 7}$$

Action potential simulations

The O'Hara-Rudy 2011 model was used to simulate the action potential (AP) of a single endocardial ventricular myocyte at 37 °C (O'Hara, 2011). The description of I_{Kr} in the O'Hara-Rudy model was replaced with the Markov state model from Lu *et al.* (Lu *et al.*, 2001), with voltage dependent gating transitions of the form $k_f = \alpha_0 \exp[z_\alpha V_m / (RT/F)]$ for forward transitions and $k_b = \beta_0 \exp[z_\beta V_m / (RT/F)]$ for backward transitions, where V_m is the membrane voltage, R is the gas constant, T is temperature and F is Faraday's constant. Peak I_{Kr} , simulated using this model was scaled to give the same peak I_{Kr} value as the original O'Hara model at 1 Hz. To examine the effect of drug binding in the context of the cardiac

MOL #103127

action potential, this Markov model was extended to include either a simple single step drug binding model, or an encounter complex drug binding model. All simulations and analysis was carried out using MATLAB software (Mathworks, Matick, MA). Simulations were equilibrated for 500 beats with a cycle length of 1000 ms.

MOL #103127

Results

Temperature dependence of steady state block of $K_v11.1$ by Cisapride

To assess the dose response relationship for cisapride block of $K_v11.1$ we measured the degree of steady state block observed at a constant holding potential of 0 mV as previously described (Hill et al., 2014). After membrane depolarization, currents were allowed to reach a stable plateau before cisapride application at concentrations between 2 and 600 nM (Figure 1). For each individual dose, cisapride was applied until steady state level of block could be measured. For example, at 22 °C the degree of block was calculated from the amplitude at the end of 100 s application for 2 nM, 10 nM, 20 nM, and 60 nM and a 20 s application for 200 and 600 nM, reflecting the shorter time required to reach steady state at higher concentrations. An example trace showing the onset of block by 60 nM cisapride during a 100 s application is shown in Figure 1A. Dose response curves were obtained in this manner for 22, 27, 32 and 37 °C (Figure 1B) and fitted with the Hill equation (Equation 3). IC_{50} values were 23.1 ± 1.1 , 17.8 ± 1.2 , 13.9 ± 1.2 and 15.4 ± 1.2 nM at 22, 27, 32 and 37°C, respectively (n = 4-7). No significant difference in IC_{50} was found between the temperatures tested (one-way ANOVA, $p > 0.05$).

Temperature dependence of kinetics of cisapride block of $K_v11.1$

A major advantage of using a high speed microfluidic exchange system to apply and washoff drug at a single holding potential is that the timecourse of block and unblock can be directly measured. To achieve this, the current decay and recovery associated with

MOL #103127

washon and washoff of cisapride were fitted with a single exponential function (Figure 2A). Typical normalized current records representing the timecourse of block and unblock of 20 nM cisapride ($\sim IC_{50}$ dose) at temperatures between 22 °C and 37 °C are shown in Figure 2B, illustrating a clear acceleration of the kinetics of both phases with increasing temperature. The measured τ values from the exponential fits indicate that the time course of both block and unblock (Figure 2C) differ significantly at higher temperatures from those measured at 22 °C ($n = 4-7$, Kruskal Wallis test, Dunn's multiple comparisons). In order to eliminate any protocol specific contribution to the measured timecourse, we compared data collected using this fast perfusion approach, with that obtained using a pre-incubation protocol (see Milnes et al., 2010). Time constants for the onset of block measured by the two methods were not significantly different (Mann Whitney test, $p > 0.05$, Supplemental Fig. 1).

We next measured the temperature dependence of the kinetics of K_v11.1 block with multiple concentrations of cisapride. The observed timecourse of block was found to be dependent on [cisapride] at all temperatures (Figure 3A), while the timecourse of washoff was independent of [cisapride] (Figure 3B) (One-way ANOVA, Tukeys multiple comparison), consistent with a simple bimolecular interaction (Scheme 1). To further interrogate the nature of the drug-channel interaction, we examined the dose dependence of the first order association rate constant (k_{on} [drug], Scheme 1) at multiple temperatures (Figure 3C). For simple diffusion limited bimolecular interactions, this relationship is linear (Fersht, 1999). While the data can be described by a straight line at 22 °C, with increasing

MOL #103127

temperature, the relationship deviates further from linear, such that higher doses blocked the channel slower than would be predicted by a linear fit to low dose data (Figure 3C). This suggests that block of $K_v11.1$ by cisapride is not diffusion limited at higher temperatures, and should be described by a more complex interaction scheme.

Modelling the temperature dependent kinetics of cisapride block

Since the data in Figure 3C suggested a simple bimolecular scheme (such as Scheme 1, Materials and Methods) is not sufficient to describe the molecular interaction between cisapride and $K_v11.1$, we introduced an intermediate encounter complex to the model (Materials and Methods, Scheme 2). This intermediate state might be interpreted as one where the drug interacts with the channel, but is yet not positioned correctly to cause conductance block. Scheme 2 was fit to idealized traces representing the timecourse of block and unblock of cisapride at multiple temperatures (Figure 4 A-D). Time constants of block and unblock measured from the simulated data are shown in comparison to experimental data in Figure 4E-F and Table 1 and 2, respectively. Critically, the non-linear relationship between $k_{on} \cdot [\text{cisapride}]$ and $[\text{cisapride}]$, calculated from the experimental data at higher temperatures, was reproduced in the values calculated from the simulated data (Figure 4G and Table 3).

MOL #103127

To further probe the mechanism of this effect, we examined the temperature dependence of the individual rate constants, k_{+1} , k_{-1} , k_{+2} and k_{-2} , from Scheme 2. This analysis showed that k_{+1} and k_{-2} were significantly temperature dependent, increasing by 9.8-fold and 4.3-fold between 22 to 37 °C (Figure 5A and D respectively). Conversely, both k_{-1} and k_{+2} only increased by ~1.9- and ~1.6-fold over the same temperature range (Fig. 5B and C respectively).

As a result of these rate changes, the equilibrium constants for the individual transitions in Scheme 2 (Materials and Methods Equations 6 and 7) had opposite temperature dependencies (Figure 5E-F). In both cases a shift in the equilibrium was observed towards the encounter complex (DC*) with increasing temperature. Specifically, K_1 shifted in the forward direction with increasing temperature (i.e. away from D + C to DC*), while K_2 shifted in the reverse direction with increasing temperature (i.e. away from DC to DC*).

This observation therefore suggests that there is a shift in the overall equilibrium towards the encounter complex with increasing temperature. We therefore examined whether altered state occupancy of the encounter complex might contribute to the non linear dose dependency of $k_{on}[\text{drug}]$ observed in Figure 3C at higher temperatures. The temperature dependencies of DC* occupancy for low dose (20 nM) and high dose (600 nM) cisapride are shown in Figure 6 A and B respectively. At low doses, DC* occupancy was never greater than 10 % regardless of temperature (between 2.6 % and 9.1 % from 22 to 37 °C, Fig. 6A). On the other hand, at higher concentrations of cisapride, the profile was quite different. At 600 nM cisapride there was significant transient accumulation of DC* between 20 % and 53

MOL #103127

% at 22 and 37 °C respectively that acts as a limiting step in the observed rate of block (Figure 6B-C). Furthermore, the maintained state occupancy of DC* explains the incomplete block of the channel observed, even at 600 nM cisapride (approximately 30 fold higher than the IC₅₀ dose). A full analysis of the temperature dependency of all state occupancies is presented in Supplemental Figure 2.

To evaluate the implications of the encounter complex model of cisapride binding to K_v11.1 in the context of the cardiac action potential, we carried out simulations using the O'Hara model of the ventricular action potential (O'Hara, 2011) (Figure 7). Within this framework we used three models to describe drug binding. First, a single step binding model with no encounter complex, where association of the drug with the channel immediately transitions to a blocked state (Figure 7Ai). In this case forward and reverse rate constants for drug binding were calculated from the timecourses of block and unblock measured for 10 nM cisapride at 37 °C from Figure 3 (using Equations 5 and 6, Materials and Methods). This model assumes that the first order rate constant scales linearly with [drug] in a diffusion limited manner, corresponding to the orange solid line in Figure 3C. Second, we implemented an encounter complex model (Figure 7Aii). In this case forward and reverse rate constants related to drug binding were those derived from the fit of Scheme 2 to our experimental data at 37 °C (Figure 5 A-D). In both cases binding to the open (O) and inactive states (I) were equivalent. Finally, we implemented a conduction block model, where I_{Kr} (the current passed through K_v11.1) was simply scaled according to the IC₅₀ curve measured at 37 °C (Figure 1B). The degree of prolongation of APD₉₀ seen in response

MOL #103127

to 20 nM cisapride was less for the encounter complex model compared to the single step model or the conduction block model (62 ms, 76 ms and 93 ms respectively (Figure 7B)). Examination of the I_{Kr} current shows that the observed difference between the encounter complex model and single step model arise from subtle difference in timing, with I_{Kr} rising slightly earlier in the former case, resulting in less prolongation (Figure 7C). Furthermore, this trend of less prolongation observed with the encounter complex model was observed over the range of concentrations tested (Figure 7D), with the difference between the two kinetic models growing at higher doses.

MOL #103127

Discussion

In this study we present the first comprehensive description of the temperature dependence of the kinetics of K_v11.1 drug block. By using a microfluidic ultrafast solution exchange system we have been able to directly measure the timecourse of block and unblock of K_v11.1 at temperatures between 22 °C and 37 °C. Our data show that the kinetics of block are significantly temperature dependent and furthermore, show complex characteristics at higher temperatures that can be explained by accumulation of drug in an intermediate encounter complex. These findings have implications for development of new preclinical screening approaches for cardiotoxic drugs and suggest that *in vitro* kinetic data needed to constrain *in silico* models for risk prediction may have to be acquired at physiological temperatures.

Complexity of block at higher temperatures

For all temperatures and concentrations of cisapride, the timecourses of both block and unblock were best described with a single exponential, consistent with a simple bimolecular interaction such as Scheme 1 (Hille, 1991). Under such a scheme, the first order association rate ($k_{on}[\text{cisapride}]$) should increase linearly with [drug]. At 22 °C this holds true, consistent with a diffusion limited process (Fersht, 1999; Holler et al., 1969). However, at higher temperatures $k_{on}[\text{cisapride}]$ is slower than would be predicted by Scheme 1 (Figure 3C), suggesting a more complex mechanism.

MOL #103127

To account for this, we considered a three state encounter complex model (Scheme 2) that has previously been used to describe many molecular interactions (Fersht, 1999; Miller, 1990) including the block of ion channels by toxins (Escobar et al., 1993, Hill et al., 2007). The encounter complex may represent any number of nonproductive drug-channel interactions that occur prior to forming the specific interactions required for block (Escobar et al., 1993). At higher temperatures more disordered movement of the drug could potentially result in a greater number or prolonged duration of these unproductive interactions, resulting in increased occupancy of the encounter complex at higher temperatures.

In silico insights into temperature- dependent block

An *in silico* model based on Scheme 2 reproduced the experimental timecourses of block and unblock (Figure 4E-F, Tables 1 and 2) as well as the non-linear concentration dependence of the first order rate constant (Figure 4G and Table 3). It should be noted that while the overall trend of the concentration dependence of $k_{on}[\text{cisapride}]$ observed experimentally was recapitulated by the model, there was some discordance for 600 nM cisapride at 37°. This occurred for two reasons. First, the experimental τ_{off} for 600 nM cisapride is slightly slower than the overall trend across doses, whereas the model has the same τ_{off} for all concentrations (see Figure 4F and Table 2). Second, the modelled τ_{on} is slightly faster than the experimentally observed time constant (Table 1). These discrepancies may be related to difficulties in accurately measuring timecourses for the highest [drug], where the onset of block is very fast (100s ms) while the timecourse of

MOL #103127

unblock may be contaminated by inefficiency in washoff related to residual drug associated with the membrane.

Overall however, there was excellent correlation between the model and the experimental data. The fitted model therefore allowed us to interrogate the individual forward and reverse rates of both the diffusion step and binding steps to yield key insights into the mechanism of block. First, in all cases, k_{+2} was not significantly faster than k_{-1} (the case at the diffusion controlled limit under this scheme (Escobar et al., 1993)) explaining the non-linearity of the first order rate constant, $k_{on}[\text{drug}]$ in Figure 3C. Second, in relation the temperature dependent observation of this effect, the rate of diffusion to the channel (k_{+1} in Scheme 2) and dissociation of the drug from the channel (k_{-2} in Scheme 2) were both highly temperature dependent, while the rates of drug binding (k_{+2} , Scheme 2) and diffusion away from the channel (k_{-1} , Scheme 2) were less affected. As a result, the equilibrium constant for the diffusion step (K_1) was increased with temperature and the equilibrium constant for the binding step (K_2) was reduced. The net effect of these changes is a transient accumulation of the encounter complex that acts as a bottleneck to the observed rate of block at higher temperatures and higher [drug].

A significant point to note is that forward rate of the ‘diffusion step’ of Scheme 2 (k_{+1}) does not purely represent diffusion of the drug through aqueous solution to the receptor site. Several observations support this. First, the model predicted rate (Figure 5A) is significantly below the supposed diffusion controlled ligand-receptor encounter frequency of $\sim 10^9 \text{ s}^{-1} \text{ M}^{-1}$ (Fersht, 1999). Second, this step is significantly temperature dependent (Q_{10}

MOL #103127

of ~ 5), while the typical Q_{10} for diffusion is ~ 1.4 (Gaede and Gawrisch, 2003; Hille, 1991; Milburn et al., 1995). One possible explanation is that the pathway to the receptor site is constrained as a result of reduced access to the channel pore by the helices that form the cytoplasmic gate for example. This access may be made less tortuous as a result of increased thermal motion as temperature is increased, thus accelerating the rate of the 'diffusion' step. Alternately, as the drug is thought to enter the channel via the cytoplasmic end of the channel pore (Kamiya et al., 2008) it must diffuse through the lipid membrane after application to the extracellular solution. Since the lipid membrane has been shown to become more fluidic with increasing temperatures (Carratu et al., 1996; Vigh et al., 1998), this potentially allows the drug to diffuse more easily at higher temperatures (Gaede and Gawrisch, 2003).

Implications for drug screening

CiPA is set to change the preclinical regulatory guidelines around how proarrhythmic risk is assigned to drugs (Fermini et al., 2015; Sager et al., 2014). Rather than using equilibrium measures of potency, that largely form the basis of existing guidelines (Food and Drug Administration, 2005), CiPA will use detailed *in vitro* assays to describe the mechanistic basis of drug binding of $K_v11.1$ and other channels, including the kinetics of drug block (Fermini et al., 2015; Sager et al., 2014). These data will then be used to constrain *in silico* models that will be used to predict proarrhythmic potential of preclinical compounds. The importance of considering the kinetics of drug/channel interaction rather than just measures of potency has been reported previously (Di Veroli et al., 2013; Lee et al., 2015)

MOL #103127

and is again highlighted by our action potential simulations (Figure 7). Both the simple single step kinetic model and the conductance block model (based on IC_{50} measures of potency) overestimated the degree of prolongation relative to an encounter complex model. This is potentially an important difference that could result in false positive hits for repolarisation prolongation in the context of *in silico* drug screening methods if accurate kinetic models are not used.

One practical hurdle that will need to be addressed is the fact that most high throughput patch clamp platforms, that will form the mainstay of the equipment for acquiring this data, operate at room temperature (Fermini et al., 2015). A key question is can this room temperature data be extrapolated to 37 °C to constrain physiologically relevant *in silico* models for risk prediction? In an ideal case, a Q_{10} value might be assigned to scale binding and dissociation rates. Our data show that, at least for cisapride, this is not the case since the dose response relationship for the timecourse of block is different at different temperatures (see Figure 3C) – meaning extrapolation may be difficult and certainly not possible using a linear scaling factor. In terms of assessing whether a set of more complex rules may exist that allow extrapolation between temperatures for a range of drugs, more studies such as this, that fully characterize temperature dependent kinetics of known blockers of $K_v11.1$ will need to be carried out. This will allow us to assess whether there is commonality in the temperature dependent binding characteristics between drugs, or whether data for individual compounds in development will simply need to be gathered at 37 °C to constrain physiologically relevant *in silico* models.

MOL #103127

Limitations

In this study we considered only a single drug binding site and did not include state dependent binding, i.e. specific kinetics of drug interaction with open and inactive states of $K_v11.1$ (Hill et al. 2014, Perrin et al. 2008, Stork et al. 2007). In previous studies of the antipsychotic clozapine, we measured fast and slow components to both block and unblock that corresponded to binding to the open and inactivated states respectively (Hill et al., 2014). For the present study, to focus on defining the mechanistic basis of temperature dependence of block, we chose a drug with simpler kinetics of interaction. For cisapride, we only ever observed a single component to block and unblock meaning we could limit consideration to a single receptor site for our analysis of temperature dependence. Reproduction of experimental time constants by the model (Figure 4) suggest this is a reasonable compromise. Future studies, involving more drugs with more complex state dependent interactions, will no doubt further the understanding of how temperature affects drug block of $K_v11.1$.

Conclusions

In summary, this study shows that the kinetics of cisapride block are temperature dependent and show complex characteristics at higher temperatures which can be explained by accumulation of drug in an intermediate encounter complex. These findings highlight the complex relationship between drug block and temperature and have significant implications for the development of new *in silico* driven approaches for assigning risk to potentially cardiotoxic drugs.

MOL #103127

Acknowledgements

The authors thank Dr Matthew Perry and Mark Hunter for informative discussion

MOL #103127

Authorship Contributions

Participated in research design: Windley, Hill, Mann, Vandenberg

Conducted experiments: Windley, Mann

Contributed to new reagents or analytical tools: Hill, Vandenberg

Performed data analysis: Windley, Mann, Hill

Wrote or contributed to the writing of the manuscript: Windley, Hill, Mann, Vandenberg

MOL #103127

References

- Barry PH (1994) JPCalc, a software package for calculating liquid junction potential corrections in patch-clamp, intracellular, epithelial and bilayer measurements and for correcting junction potential measurements. *Journal of Neuroscience Methods* **51**(1): 107-116.
- Carratu L, Franceschelli S, Pardini CL, Kobayashi GS, Horvath I, Vigh L and Maresca B (1996) Membrane lipid perturbation modifies the set point of the temperature of heat shock response in yeast. *Proceedings of the National Academy of Sciences of the United States of America* **93**(9): 3870-3875.
- Di Veroli GY, Davies MR, Zhang H, Abi-Gerges N and Boyett MR (2014) hERG inhibitors with similar potency but different binding kinetics do not pose the same proarrhythmic risk: implications for drug safety assessment. *Journal of Cardiovascular Electrophysiology* **25**(2): 197-207.
- Escobar L, Root MJ and MacKinnon R (1993) Influence of protein surface charge on the bimolecular kinetics of a potassium channel peptide inhibitor. *Biochemistry* **32**(27): 6982-6987.
- Fermini B, Hancox JC, Abi-Gerges N, Bridgland-Taylor M, Chaudhary KW, Colatsky T, Correll K, Crumb W, Damiano B, Erdemli G, Gintant G, Imredy J, Koerner J, Kramer J, Levesque P, Li Z, Lindqvist A, Obejero-Paz CA, Rampe D, Sawada K, Strauss DG and Vandenberg JI (2016) A New Perspective in the Field of Cardiac Safety Testing through the Comprehensive In Vitro Proarrhythmia Assay Paradigm. *Journal of Biomolecular Screening* **21**(1): 1-11

MOL #103127

- Fersht A (1999) *Structure and mechanism in protein science. A guide to enzyme catalysis and protein folding*. Freeman, New York.
- Food and Drug Administration H (2005) International conference on harmonisation; guidance on S7B nonclinical evaluation of the potential for delayed ventricular repolarization (QT interval prolongation). *Federal Register* **70**(1): 10.
- Gaede HC and Gawrisch K (2003) Lateral diffusion rates of lipid, water, and a hydrophobic drug in a multilamellar liposome. *Biophysical Journal* **85**(3): 1734-1740.
- Hill AP, Perrin MJ, Heide J, Campbell TJ, Mann SA and Vandenberg JI (2014) Kinetics of drug interaction with the Kv11.1 potassium channel. *Molecular pharmacology* **85**(5): 769-776.
- Hill AP, Sunde M, Campbell TJ and Vandenberg JI (2007) Mechanism of block of the hERG K⁺ channel by the scorpion toxin CnErg1. *Biophysical Journal* **92**(11): 3915-3929.
- Hille B (1991) *Ionic channels of Excitable membranes*. 2nd ed. Sinauer and Associates, Sutherland, MA.
- Holler E, Rupley JA and Hess GP (1969) Kinetics of lysozyme-substrate interactions. *Biochemical and Biophysical Research Communications* **37**(3): 423-429.
- Kamiya K, Niwa R, Morishima M, Honjo H and Sanguinetti MC (2008) Molecular determinants of hERG channel block by terfenadine and cisapride. *Journal Pharmacological Sciences* **108**(3): 301-307.
- Kirsch GE, Trepakova ES, Brimecombe JC, Sidach SS, Erickson HD, Kochan MC, Shyjka LM, Lacerda AE and Brown AM (2004) Variability in the measurement of hERG potassium channel inhibition: effects of temperature and stimulus pattern. *Journal of Pharmacological and Toxicological Methods* **50**(2): 93-101.

MOL #103127

- Lee W, Mann SA, Windley MJ, Imtiaz MS, Vandenberg JI and Hill AP (2015) In silico assessment of kinetics and state dependent binding properties of drugs causing acquired LQTS *Progress in Biophysics & Molecular Biology* **In press**.
- Lu Y, Mahaut-Smith MP, Varghese A, Huang CL, Kemp PR and Vandenberg JI (2001). Effects of premature stimulation on HERG K(+) channels. *The Journal of Physiology*, **537**(Pt 3), 843–851.
- Milburn T, Saint DA and Chung SH (1995) The temperature dependence of conductance of the sodium channel: implications for mechanisms of ion permeation. *Receptors Channels* **3**(3): 201-211.
- Miller C (1990) Diffusion-controlled binding of a peptide neurotoxin to its K⁺ channel receptor. *Biochemistry* **29**(22): 5320-5325.
- Milnes JT, Witchel HJ, Leaney JL, Leishman DJ and Hancox JC (2010) Investigating dynamic protocol-dependence of hERG potassium channel inhibition at 37 degrees C: Cisapride versus dofetilide. *Journal of Pharmacological and Toxicological Methods* **61**(2): 178-191.
- O'Hara T, Virág L, Varro A and Rudy Y (2011). Simulation of the undiseased human cardiac ventricular action potential: model formulation and experimental validation. *PLoS Computational Biology*, **7**(5), e1002061.
- Perrin MJ, Subbiah RN, Vandenberg JI and Hill AP (2008). Human ether-a-go-go related gene (hERG) K⁺ channels: function and dysfunction. *Progress in Biophysics and Molecular Biology* **98**(2-3): 137-148.
- Redfern WS, Carlsson L, Davis AS, Lynch WG, MacKenzie I, Palethorpe S, Siegl PK, Strang I, Sullivan AT, Wallis R, Camm AJ and Hammond TG (2003) Relationships between

MOL #103127

preclinical cardiac electrophysiology, clinical QT interval prolongation and torsade de pointes for a broad range of drugs: evidence for a provisional safety margin in drug development. *Cardiovascular Research* **58**(1): 32-45.

Romero L, Trenor B, Yang PC, Saiz J and Clancy CE (2014) In silico screening of the impact of hERG channel kinetic abnormalities on channel block and susceptibility to acquired long QT syndrome. *Journal of Molecular and Cellular Cardiology* **72**: 126-137.

Sager PT, Gintant G, Turner JR, Pettit S and Stockbridge N (2014) Rechanneling the cardiac proarrhythmia safety paradigm: a meeting report from the Cardiac Safety Research Consortium. *American Heart Journal* **167**(3): 292-300.

Sanguinetti MC, Jiang C, Curran ME and Keating MT (1995) A mechanistic link between an inherited and an acquired cardiac arrhythmia: HERG encodes the IKr potassium channel. *Cell* **81**(2): 299-307.

Stork D, Timin EN, Berjukow S, Huber C, Hohaus A, Auer M and Hering S (2007) State dependent dissociation of HERG channel inhibitors. *British Journal of Pharmacology* **151**(8): 1368-1376.

Vigh L, Maresca B and Harwood JL (1998) Does the membrane's physical state control the expression of heat shock and other genes? *Trends Biochemical Sciences* **23**(10): 369-374.

Walker BD, Singleton CB, Bursill JA, Wyse KR, Valenzuela SM, Qiu MR, Breit SN and Campbell TJ (1999) Inhibition of the human ether-a-go-go-related gene (HERG) potassium channel by cisapride: affinity for open and inactivated states. *British Journal of Pharmacology* **128**(2): 444-450.

MOL #103127

Wood AJ and Roden DM (2004) Drug-induced prolongation of the QT interval. *New England Journal of Medicine* **350**: 1013–1022.

Yang T, Chun YW, Stroud DM, Mosley JD, Knollmann BC, Hong C and Roden DM. (2014). Screening for Acute IKr Block Is Insufficient to Detect Torsades de Pointes Liability: Role of Late Sodium Current. *Circulation*, **130**(3), 224–234.

Yao JA, Du X, Lu D, Baker RL, Daharsh E and Atterson P (2005) Estimation of potency of HERG channel blockers: impact of voltage protocol and temperature. *Journal of Pharmacological and Toxicological Methods* **52**(1): 146-153.

Yap YG and Camm AJ (2003) Drug induced QT prolongation and torsades de pointes. *Heart* **89**(11): 1363-1372.

MOL #103127

Footnotes

This work was supported by grants from the National Health and Medical Research Council of Australia (#1088214). APH is supported by an Australian Research Council Future Fellowship (FT110100075) and JIV is supported by an NHMRC Senior Research Fellowship (#1019693).

MOL #103127

Legends for Figures

Figure 1

The effect of temperature on the potency of cisapride block of the $K_v11.1$ channel. **A**, $K_v11.1$ currents were evoked from CHO cells stably expressing $K_v11.1$ channels by stepping the membrane potential from a holding potential of -90mV to 0 mV. A typical trace representing the $I_{K_v11.1}$ evoked at 0 mV whereby a 100 s 600nM cisapride application results in current block. The maximum current (I_{max}) and maximum drug block (I_{drug}) and indicated by the closed and open circles, respectively. **B**, Concentration dependent block of $K_v11.1$ by cisapride at temperatures of 22, 27, 32 and 37 °C (green, blue, purple and orange, respectively). Percentage block of $K_v11.1$ at increasing concentrations of cisapride was calculated as the maximum current blocked following 20 to 100 s application, according to the rate at which steady state block was achieved. Data was fit with the Hill equation giving IC_{50} values of 23.1 ± 1.1 , 17.8 ± 1.2 , 13.9 ± 1.2 and 15.4 ± 1.2 nM for 22, 27, 32 and 37 °C, respectively. The IC_{50} values do not vary significantly with temperature ($p > 0.05$, one way ANOVA, and Tukey's test for multiple comparisons). The hill slope values (n_H) were also not significantly dependent on temperature ($p > 0.05$, one way ANOVA, and Tukey's test for multiple comparisons). Each data point represents the mean \pm SE of 4-8 cells.

Figure 2

The kinetics of cisapride block and unblock of $K_v11.1$ were fit by single exponentials at temperatures from 22 to 37 °C. **A**, A typical trace representing cisapride block and unblock

MOL #103127

overlayed with a single exponential fit to the rate of $I_{Kv11.1}$ block in the presence of cisapride (red broken line, τ_{on}) and unblock (blue broken line, τ_{off}). Single time constant (τ) values were calculated from these fits. **B**, Superimposed traces representing the response of $I_{Kv11.1}$ to 50 s applications of 20 nM cisapride at 22 (green), 27 (blue), 32 (purple), 37 °C (orange). Traces were normalized to maximum current block to illustrate the changes in the rate of cisapride block and unblock of $I_{Kv11.1}$. **C**, Comparison of τ values given by single exponential fits to rate of $I_{Kv11.1}$ block (red) and unblock (blue) in the presence of 20 nM cisapride at 22 to 37 °C. Each data point represents the mean \pm SE from 4-7 cells.

Figure 3

The measured τ values and calculated block rates of cisapride independent of drug concentration using a basic drug bound or drug unbound channel model. **A**, Measured τ_{on} values at different concentrations of cisapride compared at 22, 27, 32 and 37 °C (green, blue, purple and orange, respectively). **B**, Measured τ_{off} values at different concentrations of cisapride compared at 22, 27, 32 and 37 °C (green, blue, purple and orange, respectively). **C**, Summary of dose-dependency of calculated on rates (Eqn 5, $k_{on} \times [cisapride]$) of cisapride in response to 22, 27, 32 and 37 (green, blue, purple and orange, respectively). The lines represent a straight line of best fit to the data at lower concentrations cisapride. Each data point represents the mean \pm SE from 4-7 cells.

Figure 4

Comparison of the encounter complex model to the experimental data. **A-D**, Fits of the encounter complex model to the averaged experimental data. Traces have been overlayed

MOL #103127

representing mean of 4-7 experiments (solid line) \pm SE (broken line) at 10 (green), 20 (blue), 60 (purple), 200 (orange), and 600 nM (red). Fit of scheme 2 to the experimental data is shown as a black line overlaying the coloured experimental data. Data is shown at 22 (A), 27 (B), 32 (C) and 37 °C (D). E-F Comparison of the measured τ_{on} (E) and τ_{off} (F) values from the experimental (circles) and model (line) data. G, Summary of apparent concentration dependency of the calculated on rate ($k_{on} \times [cisapride]$) of cisapride from the modeled fit, data for 22, 27, 32 and 37 °C are represented in green, blue, purple and orange, respectively). The line represents a straight-line of best fit through the data points at lower concentrations of cisapride.

Figure 5

Temperature dependency of cisapride diffusion and binding rates to Kv11.1, according to scheme 2. A-B Rates of transition between the D + C and the DC* state, where k_{+1} (A) is the forward rate and k_{-1} (B) the reverse rate. C-D, Rates of transition between the DC* and the DC state, where k_{+2} (C) is the forward rate and k_{-2} (D) the reverse rate All rates were calculated from the encounter complex modeling (scheme 2) fits and plotted at each temperature tested. C-D Calculated equilibrium constants for the transition from D + C to DC* (C, Eqn 6) and DC* to DC (D, Eqn 7).

Figure 6

Predictions of DC* and DC occupancy calculated from scheme 2 during cisapride block to illustrate the accumulation of drug in DC* and the subsequent impact on DC occupancy at high concentrations. (A-B) Percentage occupancy of DC* in the first 5 s of block in response

MOL #103127

to 20nM **(A)** and 600nM **(B)** cisapride at 22 (green), 27 (blue), 32 (purple) and 37 °C (orange). **(C)** Summary of DC occupancy in the first 5 s of cisapride block in response to 20 nM (broken lines) and 600 nM cisapride (solid lines) in response to 22, 27, 32 and 37 °C (green, blue, purple and orange, respectively).

Figure 7

Simulations of action potential prolongation by cisapride block of K_v11.1. A) Markov state models used to describe block of K_v11.1 by cisapride. Parameters related to state transitions are summarized in Table 4. B) Simulation of action potentials prolongation in response to 20 nM cisapride. APD₉₀s were 330 ms, 392 ms, 406 ms and 423 ms for control, the encounter complex model, the single step binding model and conductance block model respectively. C) I_{Kr} currents corresponding to the action potentials shown in (B). D) APD₉₀ prolongation

Tables

Table 1: Comparison of experimental and model derived timecourse of cisapride block of K_v11.1 at 22 to 37 °C

	Cisapride τ_{on} (s ⁻¹)									
	10 nM		20 nM		60 nM		200 nM		600 nM	
	Experiment	Model	Experiment	Model	Experiment	Model	Experiment	Model	Experiment	Model
22 °C	27.8 ± 1.6	30.1	20.4 ± 1.7	23.1	8.6 ± 1.3	12.1	5.6 ± 0.7	4.7	2.3 ± 0.3	2.0
27 °C	14.0 ± 1.0	16.3	9.6 ± 0.6	12.0	4.6 ± 0.8	6.0	2.0 ± 0.1	2.4	1.2 ± 0.2	1.1
32 °C	8.2 ± 1.0	8.9	5.4 ± 0.4	6.3	3.4 ± 0.3	3.0	1.2 ± 0.1	1.3	0.8 ± 0.1	0.7
37°C	5.1 ± 0.3	4.9	4.6 ± 0.5	3.4	3.2 ± 0.4	1.6	1.0 ± 0.01	0.7	0.9 ± 0.1	0.4

Table 2: Comparison of experimental and model derived timecourse of recovery from cisapride block of K_v11.1 at 22 to 37 °C

	Cisapride τ_{off} (s ⁻¹)									
	10 nM		20 nM		60 nM		200 nM		600 nM	
	Experiment	Model	Experiment	Model	Experiment	Model	Experiment	Model	Experiment	Model
22 °C	38.7 ± 1.7	43.2	42.0 ± 5.5	43.2	38.1 ± 5.3	43.2	45.0 ± 4.2	43.2	50.9 ± 5.8	43.2
27 °C	26.1 ± 2.5	25.4	25.2 ± 2.3	25.4	26.2 ± 3.2	25.4	26.8 ± 3.2	25.4	30.9 ± 1.6	25.4
32 °C	14.5 ± 2.0	15.2	14.1 ± 2.1	15.2	14.1 ± 1.2	15.2	17.4 ± 1.2	15.2	17.5 ± 2.1	15.2
37 °C	9.4 ± 0.7	9.3	10.6 ± 0.5	9.3	9.3 ± 0.8	9.3	10.5 ± 1.6	9.3	13.5 ± 2.2	9.3

Table 3: Comparison of experimentally and model derived first order association rate constants for binding of cisapride to K_v11.1 at 22 to 37 °C

	$k_{on} \cdot [\text{cisapride}] \text{ (s}^{-1}\text{)}$									
	10 nM		20 nM		60 nM		200 nM		600 nM	
	Experiment	Model	Experiment	Model	Experiment	Model	Experiment	Model	Experiment	Model
22°C	0.010 ± 0.002	0.010	0.025 ± 0.002	0.020	0.098 ± 0.02	0.060	0.167 ± 0.02	0.191	0.452 ± 0.06	0.486
27°C	0.029 ± 0.007	0.022	0.060 ± 0.010	0.044	0.138 ± 0.02	0.128	0.463 ± 0.04	0.386	0.878 ± 0.11	0.865
32°C	0.054 ± 0.008	0.047	0.111 ± 0.019	0.092	0.219 ± 0.02	0.265	0.796 ± 0.09	0.737	1.195 ± 0.14	1.45
37°C	0.092 ± 0.011	0.096	0.137 ± 0.022	0.188	0.254 ± 0.05	0.518	0.915 ± 0.01	1.27	1.065 ± 0.13	2.14

MOL #103127

Table 4.

Table 4: Summary of parameters related to Markov models in Figure 7.

Gating transitions				
	α_0	z_α	β_0	z_β
$C_0 - C_1$	0.1161	0.299	0.2442	-1.604
$C_1 - C_2$	0.1235	0	0.1911	0
$C_2 - O$	0.0578	0.971	0.000349	-1.062
$C_2 - I$	0.000052	1.525	0.0000000085	-1.842
$O - I$	0.2533	0.5953	0.0522	-0.8209
Drug binding transitions				
	Single step binding model		Encounter complex model	
	k_f	k_b	k_f	k_b
$O - OD / I - ID$	8418884	0.10654		
$O - OD^* / I - ID^*$			12540100	0.9697
$OD^* - OD / ID^* - ID$			2.805	0.454774

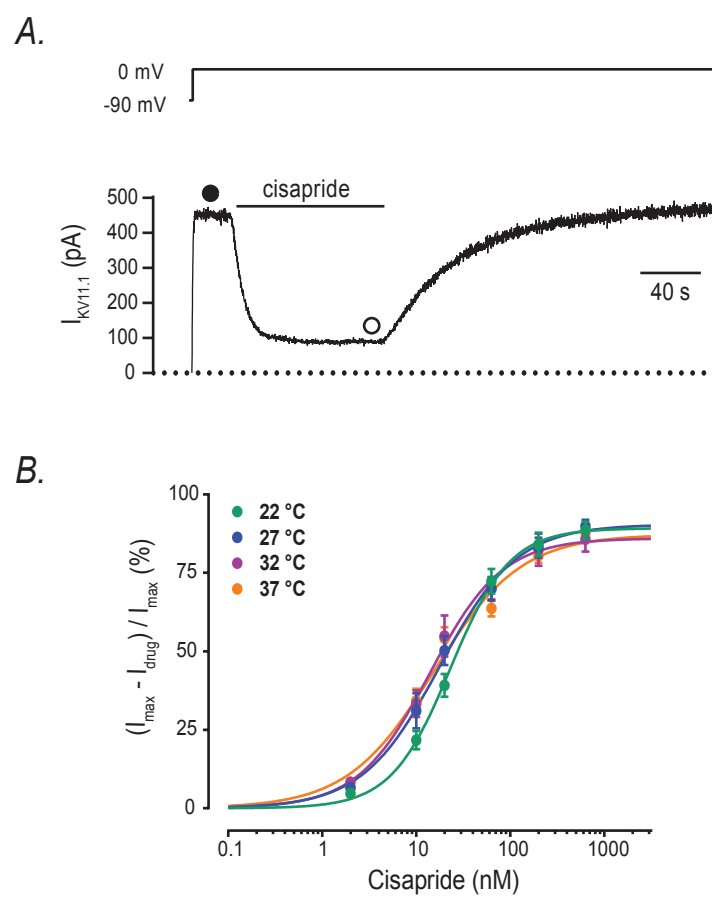


Figure 1

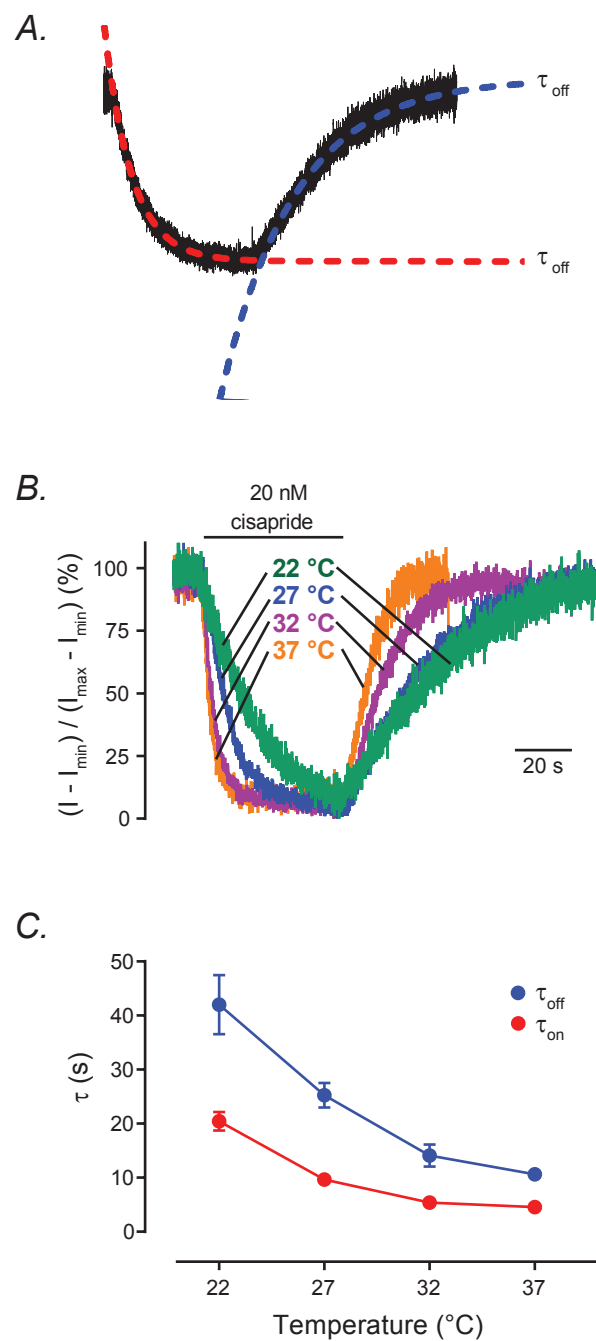


Figure 2

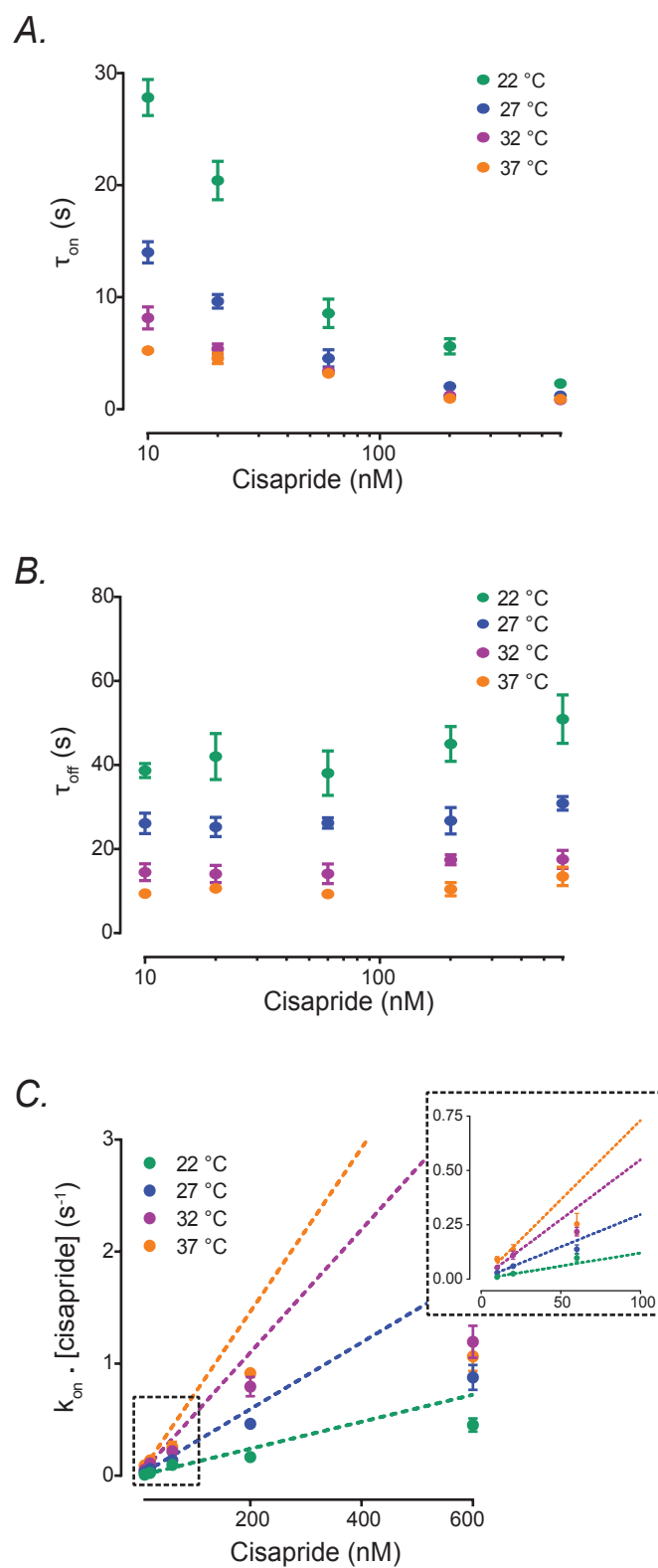


Figure 3

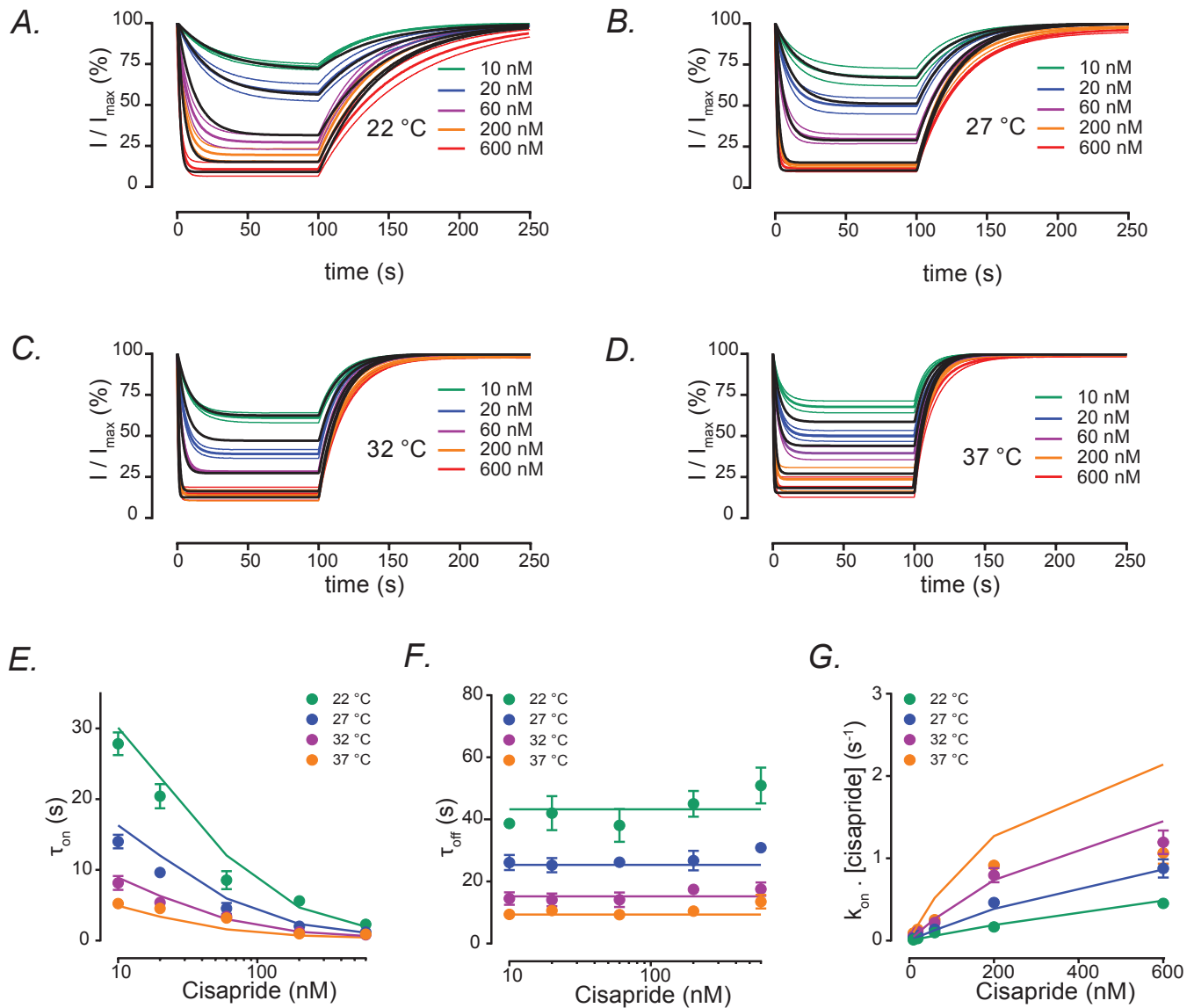


Figure 4

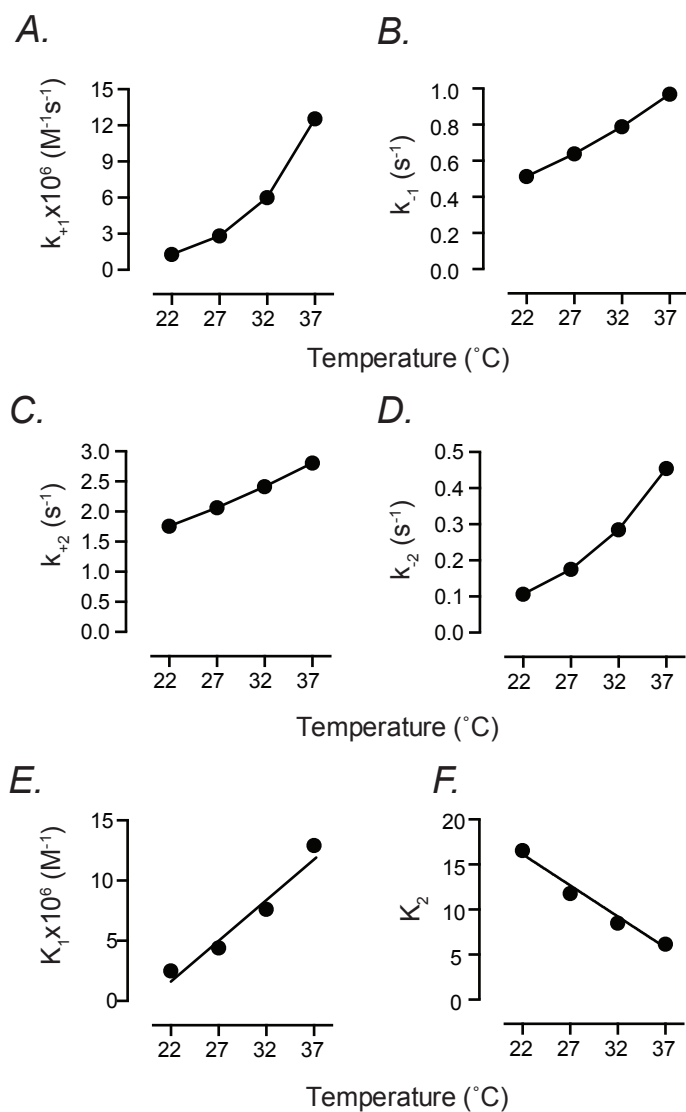


Figure 5

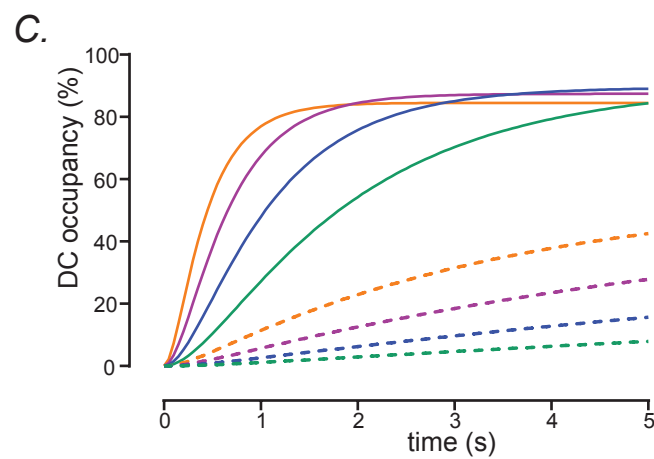
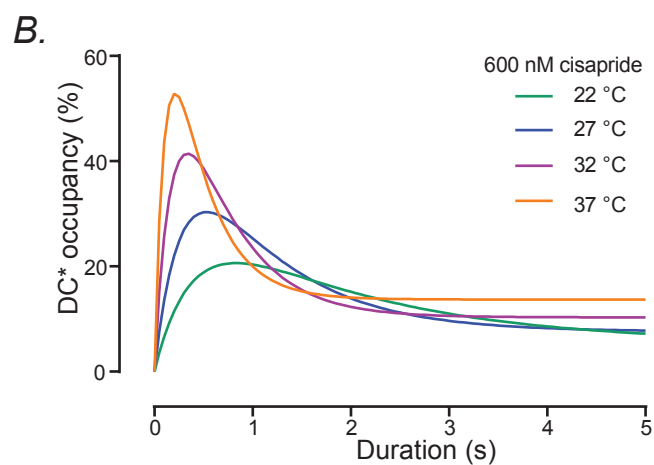
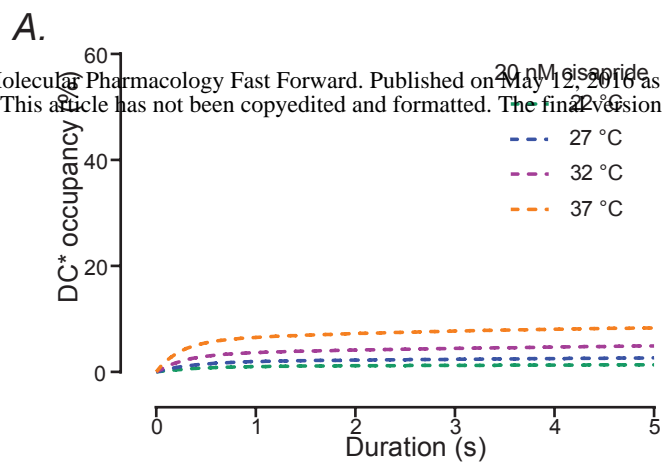


Figure 6

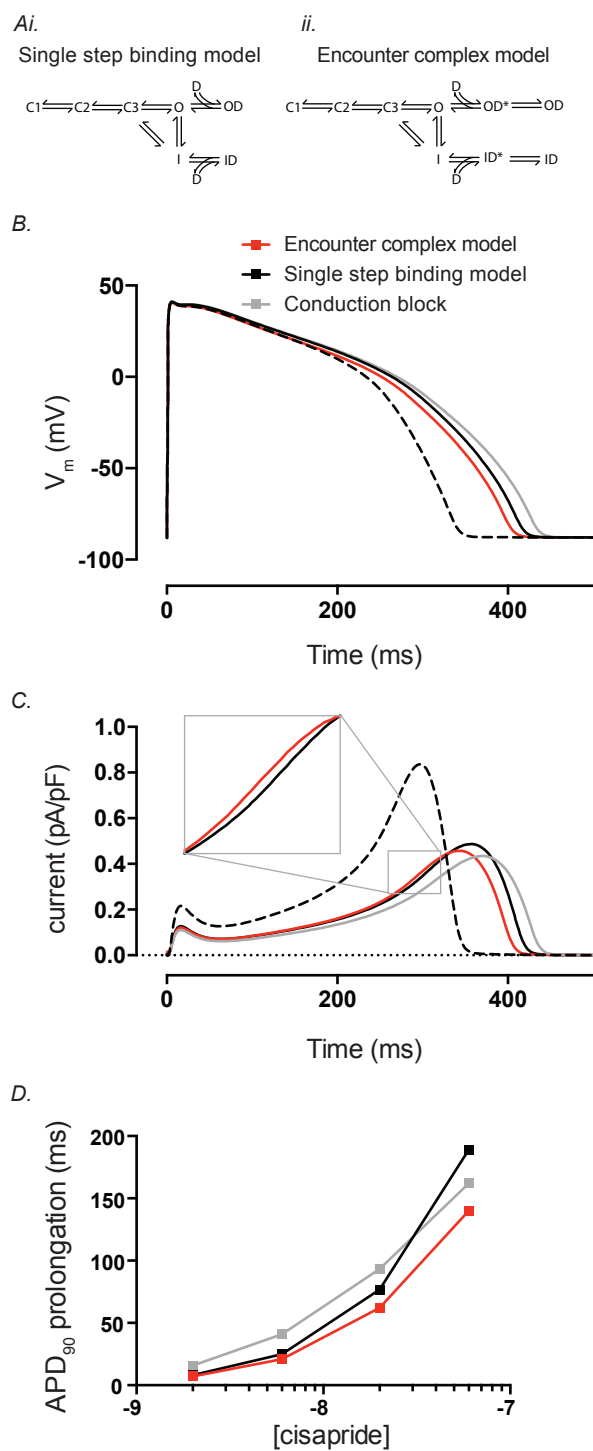


Figure 7